



## ANTIBACTERIAL ACTIVITY OF INTRACELLULAR GREENLY FABRICATED SELENIUM NANOPARTICLE OF *Lactobacillus pentosus* ADET MW861694 AGAINST SELECTED FOOD PATHOGENS

 Bukola Christianah Adebayo-Tayo<sup>1+</sup>  
 Bola Olawunmi Yusuf<sup>2</sup>  
 Solomon Omoniyi Alao<sup>3</sup>

<sup>1,2,3</sup>Department of Microbiology, University of Ibadan, Ibadan, Oyo State, Nigeria.

<sup>1</sup>Email: [bukola.tayo@gmail.com](mailto:bukola.tayo@gmail.com) Tel: +234 8035522409

<sup>2</sup>Email: [yusufbola1002066@yahoo.com](mailto:yusufbola1002066@yahoo.com)

<sup>3</sup>Email: [omonyialao02@gmail.com](mailto:omonyialao02@gmail.com)



(+ Corresponding author)

### ABSTRACT

#### Article History

Received: 25 May 2021

Revised: 17 June 2021

Accepted: 13 July 2021

Published: 3 August 2021

#### Keywords

*Lactobacillus pentosus*  
Selenium nanoparticles  
Food  
Foodborne pathogens  
Antagonistic  
*Salmonella arizonae*.

This study aimed at intracellular biosynthesis of selenium nanoparticles using *Lactobacillus pentosus*ADEB (LP) and the greenly fabricated nanoparticles were characterized based on visual observation, spectroscopy, microscopy, energy dispersive X-rays, X-ray Diffraction, and dynamic light scattering properties. The antibacterial activities of the *Lactobacillus pentosus*ADEB selenium nanoparticles (LP-SeNPs) against selected foodborne pathogens were evaluated. A gradual change in colour from brown to reddish colour indicates the formation of Nano-selenium. The highest absorption peak for LP-SeNPs was visible between 200-300nm. FTIR analysis shows major peaks around 1635.40, 1587.31 2163.00, 2936.70, 2968.50, and 3254.38 cm<sup>-1</sup> indicate the presence of amides on the nanoparticle surface. SEM and TEM analysis shows extrusion of spherical shape SeNPS from *Lactobacillus pentosus* cell membrane which indicates intracellular synthesis of the nanoparticles. The nanoparticles were crystalline with an average diameter of 106.1 nm and a polydispersity index of 0.295. Elemental selenium with an absorption peak at 1.37 Kev was present in the nanoparticles. The LP-SeNPs and culture of *Lactobacillus pentosus* had antagonistic activities against the foodborne pathogens. The LP-SeNPs have antagonistic activity against all the test pathogens. The highest activity was against *Salmonella arizonae* (11.3 mm). In conclusion, the intracellular greenly fabricated LP-SeNPs had broad-spectrum antagonistic activity against the test food-borne pathogens. The addition of selenium nanoparticles to food can be an added advantage in controlling food-borne pathogens.

**Contribution/Originality:** This study contributes to existing literature by using green route for intracellular biosynthesis of selenium nanoparticle using *Lactobacillus pentosus* ADET MW861694 and by analyzing the antibacterial potential of the fabricated nanoparticles against some food pathogens. This study uses new estimation methodology for characterization of the fabricated selenium nanoparticles.

### 1. INTRODUCTION

Spoilage of food through the activities of microorganisms which resulted in a reduction in shelf-life which can result in an increase in food-borne infection and intoxication and probably shortage of food is a serious global concern. The outbreak of food-borne infection and intoxication possess a serious health threat to the populace all over the world. The search for newer antimicrobials with dual functions to serve as an antagonistic agent and

nutrient enrichment and fortification in the food industry resulted in the emergence of nanotechnology in this research area. The concept of nanotechnology involves the manipulation of substances and materials at the molecular level for the production of particles and structures with a nanoscale (ranges from 1-100nm) generally regarded as Nanoparticles. Nanoparticles show uniqueness in properties such as high surface to volume ratio, mechanical strength, light absorption, thermal and electrical conductivity, an active surface that has relevant photocatalytic properties, and electrostatic interaction with bioactive compounds in their environment (Kato, 2011; Xiao & Wiesner, 2012; Xie, He, Irwin, Jin, & Shi, 2011). Several types of nanoparticles such as silver (Ag) nanoparticles, gold (Au) nanoparticles, copper (Cu) nanoparticles have been developed using biological benign (Gericke & Pinches, 2006). The use of microorganisms, their metabolites, and plants for the bio-reduction of metal ions is based on their ability to absorb and accumulate inorganic metal ions from the surrounding environment. Bacteria, fungi, and Algae have been reportedly used for nanoparticle biosynthesis (Adebayo-Tayo, Salaam, & Ajibade, 2019; Korbekandi, Iravani, & Abbasi, 2012; Korbekandi, Ashari, Iravani, & Abbasi, 2013; Mokhtari et al., 2009; Vigneshwaran et al., 2007).

Selenium has been reported as an essential trace metal and a dietary food supplement with immune-regulative, fertility-promoting, anti-carcinogenic, anti-aging, antioxidant, detoxification, and antibacterial activity (Li, Yi, Jun, Huigang, & Songsheng, 2002; Mater et al., 2005; Navarro-Alarcon & López-Martinez, 2000). Selenium has a recommended dietary allowance for adults of 55 µg/d (tolerable upper level is 400 µg/d) and it plays a crucial role in human health (Institute of Medicine, 2000). Lactic acid bacteria (LAB) are Generally Recognized as Safe Status (GRAS). The combination of selenium and LAB as an antagonistic agent both in-vitro and in-vivo has been reported to have a better synergetic effect compared to the effect of selenium or lactic acid bacteria alone (Yang et al., 2009). The potential of Selenium fortified LAB as a novel antimicrobial agent against foodborne pathogens in fermented food can be harnessed. A Se-enriched dairy product as a potent functional food to satisfy the need for selenium utilization and provide a solution to the selenium deficiency problem in certain areas (Alzate et al., 2007; Alzate, Fernández-Fernández, Pérez-Conde, Gutiérrez, & Cámara, 2008; Alzate, Pérez-Conde, Gutiérrez, & Cámara, 2010; Palomo, Gutiérrez, Pérez-Conde, Cámara, & Madrid, 2014) has been reported. Easy generation of absorbable and high-nutritive organic Se by some microorganisms such as *Lactobacillus brevis*, *Lactobacillus bulgaricus*, *Enterococcus faecium*, *Enterococcus durans*, *Lactococcus lactis* ssp. *Lactis*, *Lactobacillus rhamnosus*, and *Lactobacillus fermentum* through biotransformation during fermentation has been reported (Andreoni, Luischi, Cavalca, Erba, & Ciappellano, 2000; Deng et al., 2015; Guo et al., 2013; Mego et al., 2005; Pieniz, Andrezza, Pereira, de Oliveira Camargo, & Brandelli, 2013; Xia, Chen, & Liang, 2007). There is a dearth of information on biosynthesis of selenium nanoparticles of *Lactobacillus pentosus* as antimicrobials to combat food-borne pathogens.

The majority of food-borne diseases etiological agents are pathogens from the genera Salmonella, Listeria, Escherichia, staphylococci, Clostridium, and Campylobacter. Hence a continuous search for potent antimicrobials that can function at different stages of food processing, nutrient augmentation, and packaging is needed. Thus this study aimed at intracellular biosynthesis and characterization of selenium nanoparticles using *Lactobacillus pentosus* ADEB (LP) and evaluation of its antibacterial potential against selected foodborne pathogens.

## 2. MATERIALS AND METHODS

### 2.1. Collection and Activation of Culture

Probiotic *Lactobacillus pentosus* ADET MW861694 culture previously isolated from “wara” and five foodborne pathogens (*Escherichia coli*, *Salmonella arizola*, *Salmonella typhi* ATCC 14028, *Staphylococcus aureus* ATCC 25923, and *Staphylococcus aureus* 16<sub>6</sub>) were obtained from the Culture Collection, Microbial Physiology Unit, Department of Microbiology, University of Ibadan, Ibadan, Nigeria. The LAB isolate was cultivated in sterile MRS broth at 37°C for 48 hrs and further activated in sterile de Man Rogosa and Sharpe (MRS) agar for 48hours at 37°C. Following incubation, the colonies were enumerated by plate count method until their population reached

approximately  $10^8$ – $10^9$  Colony Forming Units per milliliter (CFU/mL). *Escherichia coli*, *Salmonella arizola*, *Salmonella typhi* ATCC 14028, *Staphylococcus aureus* ATCC 25923, and *Staphylococcus aureus* 16<sub>6</sub> were inoculated in sterile Nutrient broth and incubated at 37°C for 24 hours. Pure and distinct colonies of these isolates were then aseptically sub-cultured on 10 mL of freshly prepared sterile nutrient agar and incubated at 37°C for 12 hrs (Yang et al., 2009).

### 2.2. Intracellular Green Synthesis of Selenium Nanoparticles Using *Lactobacillus pentosus*

Intracellular biosynthesis of SeNPs using *L. pentosus* was done according to the method of Deng et al. (2015). 10 mL of the seed culture was aseptically inoculated into 100 mL of sterile MRS broth and incubated at 37°C for 48 hours. 50 mL of the fermentation broth was centrifuged at 4,000×g for 15 minutes to separate the pellet (culture) from the supernatant. The pellet from the centrifuged fermentation broth was added to 500 mL MRS broth seeded with the most suitable selenite concentration (5 mM) and incubated at 37°C for 72 hours.

### 2.3. Characterization of the Greenly Synthesized Selenium Nanoparticles

The greenly synthesized intracellular SeNPs using *L. pentosus* was characterized using:

#### 2.3.1. Visual Observation

The gradual changes in colour of the culture medium with or without sodium selenite were monitored and observed visually.

#### 2.3.2. UV-Visible Spectroscopy

This was done to determine the optical properties of the greenly synthesized LP-SeNPs. 2 mL of the LP-SeNPs samples cultured at 24–72 hrs were scanned between 200 and 700 nm wavelength, with a resolution of 1 nm. The UV-Visible spectra were recorded at different intervals of 24–72 hrs (Alkammash, 2017).

#### 2.3.3. Fourier Transform Infrared Spectroscopy (FT-IR)

The LP-SeNPs were dried and diluted with potassium bromide (FT-IR grade) in the ratio of 1:100. The FT-IR spectrum of samples was recorded on an FT-IR spectrophotometer (Jasco FT/IR-6300) equipped with JASCO IRT-7000 Intron Infrared Microscope. The spectrum was recorded in the wavenumber range of 350–4,000  $\text{cm}^{-1}$  at a resolution of 4  $\text{cm}^{-1}$  and analyzed by subtracting the spectrum of pure KBr. The peaks obtained were plotted as transmittance in Y-axis and wavenumber ( $\text{cm}^{-1}$ ) in X-axis (Saifuddin, Wong, & Yasumira, 2009).

#### 2.3.4. Scanning Electron Microscopy (SEM)

The morphological characteristics of nanoparticles were determined using SEM. The precipitate from the centrifuged LP-SeNPs was dispersed in sterile water, washed twice and the pellet was carbon coated on a copper grid, dried, and subjected to SEM analysis using Phenom ProX Scanning Electron Microscope. The details regarding applied voltage, magnification used, and size of the contents of the image were also implanted on the images.

#### 2.3.5. Transmission Electron Microscopy (TEM)

TEM analysis of the LP-SeNPs was done by dropping the purified pellet on a carbon-coated grid, dried and the TEM analysis was performed by using JOEL JCM-7000 instrument operated at an accelerating voltage of 15kV with a resolution of 0.23 nm (Gericke & Pinches, 2006).

### 2.3.6. Energy Dispersive X-ray (EDX)

The elemental composition of LP-SeNPs was determined using EDX. The pellet from the centrifuged LP-SeNPs samples was dried. 100nm thick section of the pellet was placed on the grid and analyzed using Rigaku instrument model NEX CG. Pure selenium standard was used for calibration, and then a working curve was selected according to the sample. The sample was then tested and the result outputted (Scimeca, Bischetti, Lamsira, Bonfiglio, & Bonanno, 2018).

### 2.3.7. X-Ray Diffraction (XRD)

The crystalline nature of the greenly synthesized LP-SeNPs was determined using XRD. A slurry of the dehydrated LP-SeNPs samples was placed in a quartz disk. The disk was placed on an XRD slit and analyzed using an X-ray diffractometer (Malvern Zetasizer, Nano Z500 UK) in the region of  $2\theta$  operating at a voltage of 45kV and a current of 30mA at room temperature (Ghareib, Tahon, Saif, & Abdallah, 2016).

### 2.3.8. Dynamic Light Scattering (DLS)

DLS was used to determine the size distribution profile of LP-SeNPs. Pellet from centrifuged LP-SeNPs was diluted in sterile distilled water. The diluted samples were analyzed using a DLS system (Malvern Zetasizer, Nano Z500 UK) and the temperature of the medium was maintained at 25°C.

### 2.3.9. Antibacterial Potential of the Intracellularly Synthesized LP-SeNPs and Cell-Free Culture Supernatants (CFCS) Obtained from LP-SeNPs

The antibacterial activity of the intracellularly synthesized LP-SeNPs and CFCS was determined using the Agar Well Diffusion Method (Shivashankar, Premkumari, & Chandan, 2013). *E. coli*, *S. arizonae*, *S. tyhimurium* ATCC 14028, *S. aureus* ATCC 25923, and *S. aureus* 16<sub>6</sub> was used as the test pathogens. The isolates were cultured overnight on nutrient agar plates. McFarland standard of the 18 hours old culture of the test pathogens was seeded on Mueller-Hinton Agar (Oxoid Ltd., England) plates. Uniform wells were cut on the dried agar plate using a sterile cork-borer of 5 mm. Each well was filled with 20  $\mu$ L of the bacterial cultures and CFCS obtained from LP-SeNPs and *L. pentosus*. Sodium selenite (5 mM) was used as a negative control. The inoculated plates were incubated at 37°C for 24 hrs. After incubation, the plates were observed for zones of inhibition around the wells. Zones of inhibition diameter greater than 1 mm were considered positive (Prabhu, Mohan, Sanhita, & Ravindran, 2014).

## 3. RESULTS

### 3.1. Intracellular Green Synthesis of Selenium Nanoparticles Using *Lactobacillus Pentosus*

The visual observation of the LP-SeNPs greenly synthesized using sodium selenite after 72 hours of incubation is shown in Figure 1. Changes in colour from light yellow to deep red were observed in the reaction medium.



Figure-1. Visual Characterization of LP-SeNPs at 72hrs.

Keys: A - 5mM Sodium selenite, B - Broth and Sodium selenite mixture.  
C - LP-SeNPs.

### 3.2. Characterization of the Greenly Synthesized Selenium Nanoparticles

#### 3.2.1. UV-Visible Spectroscopy

The UV-Visible spectra of the biosynthesized LP-SeNPs at different incubation time is shown in Figure 2. At 24, 48, and 72 hrs of incubation, a sharp Surface Plasmon Resonance (SPR) peak was observed at 250 nm and 300 nm.

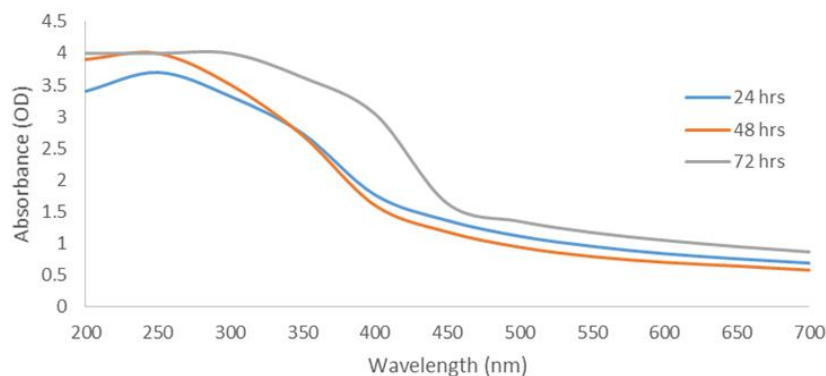


Figure-2. UV-Vis Absorption Spectra of LP-SeNPs at Different Hours of Production.

#### 3.2.2. Fourier Transform Infrared Spectroscopy (FT-IR)

The FT-IR spectrum of the greenly synthesized LP-SeNPs is shown in Figure 3. Twenty-six peaks were observed starting from 3254.38  $\text{cm}^{-1}$  to 368.84  $\text{cm}^{-1}$ . The most prominent bend at 3254.38  $\text{cm}^{-1}$  could be attributed to -OH broad stretch of alcohol. The absorption peak at 2968.50  $\text{cm}^{-1}$  and 2936.70  $\text{cm}^{-1}$  could be  $\text{SP}^3$  C-H stretches. The peak at 2163.00  $\text{cm}^{-1}$  indicates the carbonyl stretching of transition metals. The absorption peak at 1635.40  $\text{cm}^{-1}$  and 1587.31  $\text{cm}^{-1}$  corresponds to the C=C stretch of an aromatic ring where there is a delocalized electron system. The absorption peak at 1412.22  $\text{cm}^{-1}$  indicates the presence of the C-C bend of aldehyde. The peak at 1122.55  $\text{cm}^{-1}$  is characteristic of the C-N stretch of an aliphatic amine. The peak at 1084.00  $\text{cm}^{-1}$  indicates the presence of Alkyl aryl ether (C-O). The absorption peak at 1042.66  $\text{cm}^{-1}$  could be attributed to the presence of the C-O functional group of esters and phenol. The weak peak at 992.72  $\text{cm}^{-1}$  indicates the presence of the alkane (C=C) group. The peak at 923.67  $\text{cm}^{-1}$  corresponds to vibrations of out of plane CH. The weak peak at 853.87  $\text{cm}^{-1}$  could be attributed to the presence of the aromatic CH functional group. The medium peak at 774.51  $\text{cm}^{-1}$  corresponds to vibrations of the alkene (C=C) group. Furthermore, the peak at 651.52  $\text{cm}^{-1}$  and 619.55  $\text{cm}^{-1}$  indicates the presence of the Alkyl (C-Br) group while the peak at 555.23  $\text{cm}^{-1}$  indicates the presence of the alkyl (C-L) group. The peak at 435.94  $\text{cm}^{-1}$  and 416.18  $\text{cm}^{-1}$  correspond to the Aryl disulfides (S-S) group.

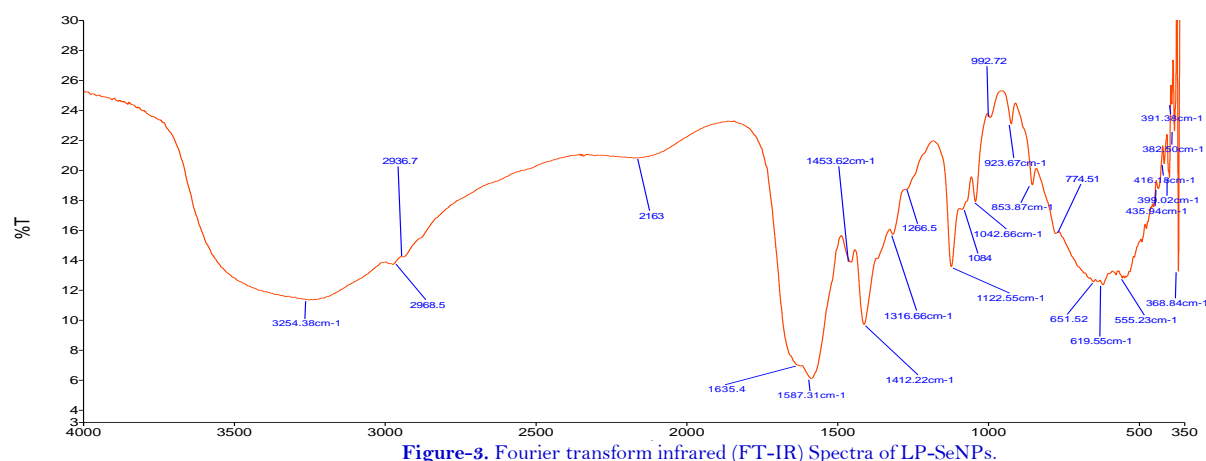


Figure-3. Fourier transform infrared (FT-IR) Spectra of LP-SeNPs.

3.2.3. Microscopy

SEM analysis of greenly synthesized LP-SeNPs is shown in Figure 4. Figure 4a shows the spherical LP-SeNPs around the outer cell membrane while Figure 4b shows the LP-SeNPs to agglomerate in the surrounding medium. Figure 5. Shows TEM of the intracellularly deposited spherical LP-SeNPs.

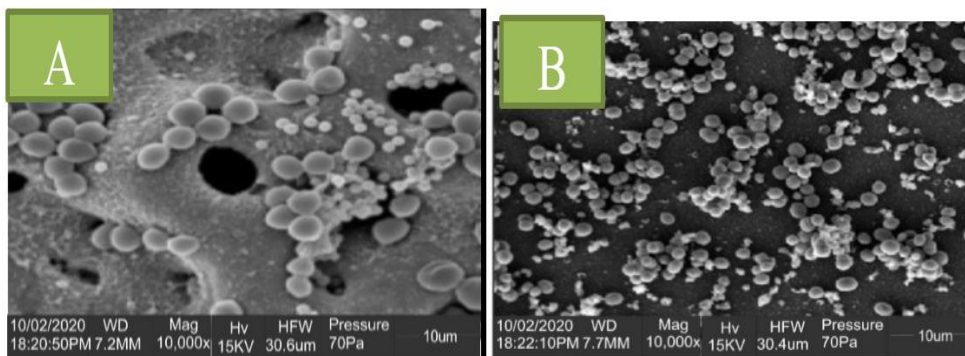


Figure-4a-b. Scanning Electron Micrograph of LP-SeNPs. A - SeNPs around the outer membrane of *Lactobacillus pentosus* NRIC 0391; B - *Lactobacillus pentosus* ADETMW861694 SeNPs agglomerate in the surrounding medium.



Figure-5. Transmission Electron Micrograph of Intracellular Deposits of Bioreduced LP-SeNPs.

3.2.4. Energy Dispersive X-ray (EDX)

The EDX spectrum ascertains the presence of selenium in the sample as shown in Figure 6. The presence of other elements is attributed to grid support. The EDX spectrum shows that the selenium atom (24.8%) was present, and the characteristic energy level at 1.50 keV.

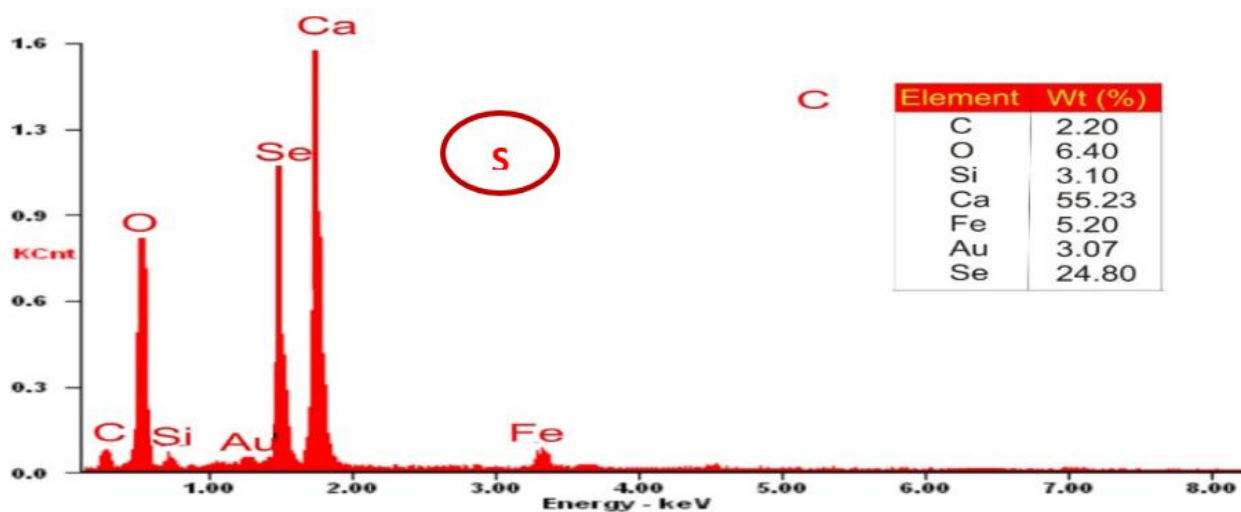


Figure-6. EDX Spectra of Greenly Synthesized LP-SeNPs.

### 3.2.5. X-Ray Diffraction (XRD)

X-ray Diffraction spectra shown in Figure 7 provide information about crystalline phases of the selenium nanoparticles. The figure shows X-Ray Diffraction of the greenly synthesized LP-SeNPs at a  $2\theta$  angle of 0–80°. Five diffraction peaks were present starting from 6.6916° to 23.9124°. The diffraction peaks at the position of  $2\theta$  values of 6.6916°, 19.7324°, 21.0314°, 21.7120°, and 23.9124° correspond to 110, 322, 331, 420, and 422 planes of the face-centered cubic (FCC). This indicates that the greenly synthesized selenium nanoparticles have a crystalline nature. The peaks observed in the XRD spectrum confirmed that selenium nanoparticles have been formed in the form of nanocrystals. The diffraction peaks at position  $2\theta$  values of 6.6916°, 19.7324°, 21.0314°, 21.7120°, and 23.9124° correspond to 110, 322, 331, 420, and 422 planes of the face-centered cubic (FCC).

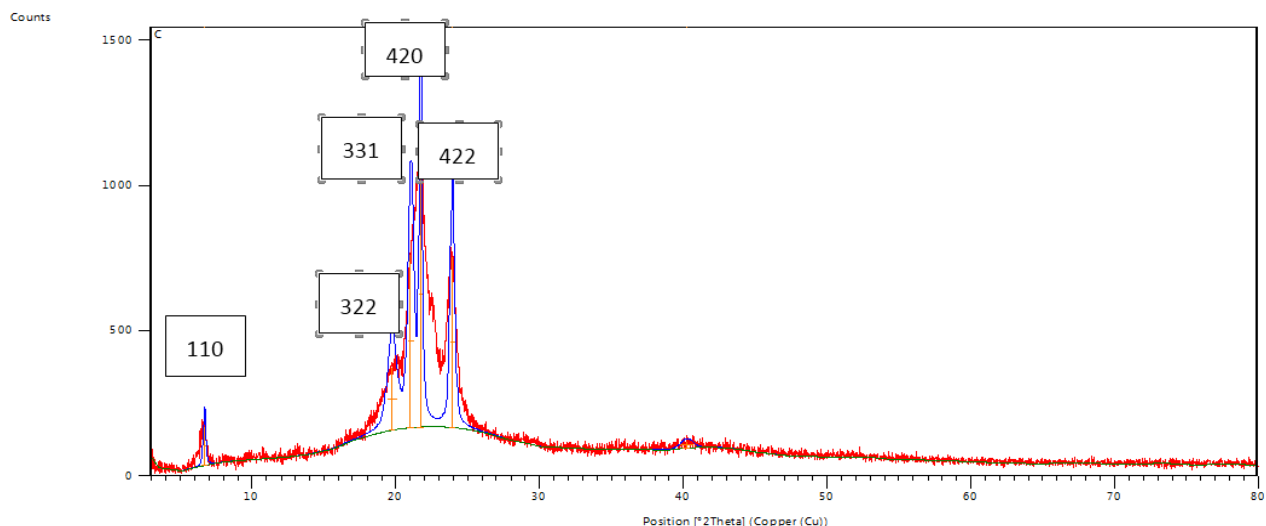
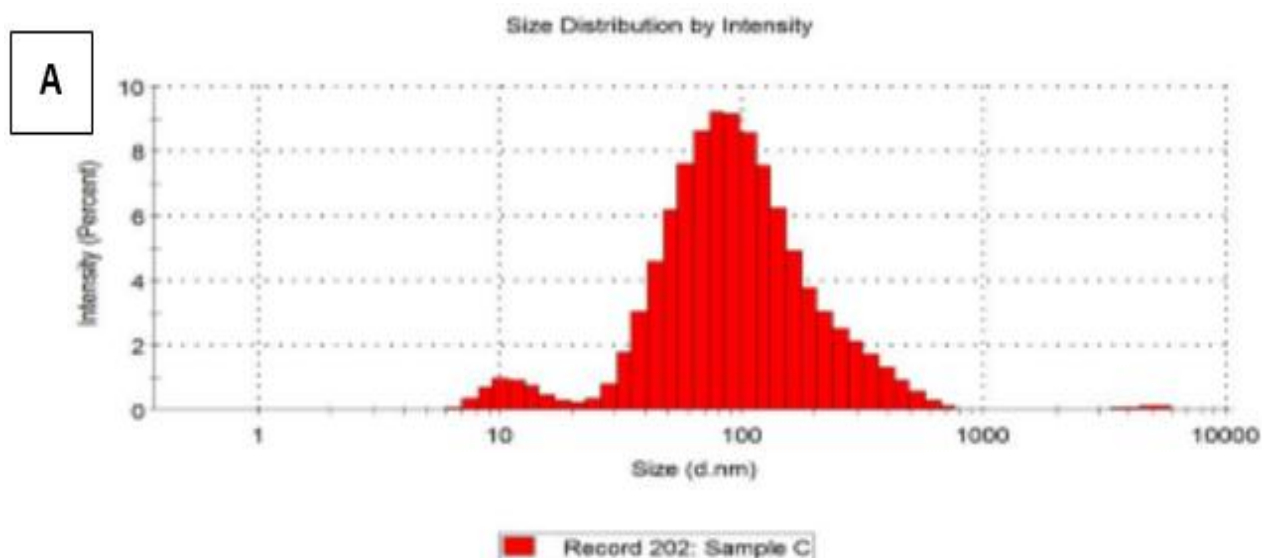


Figure-7. XRD spectra of Greenly Synthesized LP-SeNPs.

### 3.2.6. Dynamic Light Scattering (DLS)

Figure 8a-b reports the particle average diameter size, size distribution, and polydispersity index (PDI) of the greenly synthesized LP-SeNPs using Dynamic Light Scattering. The DLS spectrum shows the average diameter size to be 106.1 nm and a polydispersity index of 0.295.



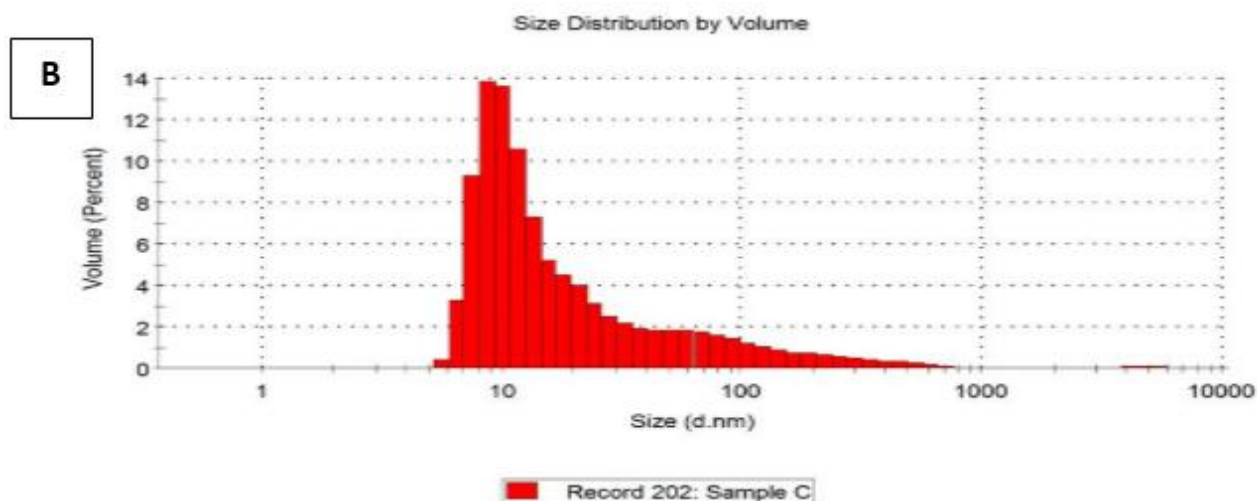


Figure-8b. DLS Spectra of Greenly Synthesized LP-SeNPs. A - Size Distribution by Intensity; B - Size Distribution by Volume.

### 3.3. Antibacterial Potential of the Intracellularly Synthesized LP-SeNPs and LP-Culture against the Test Pathogens

The antagonistic activity of LP-SeNPs against the food-borne pathogen is shown in Table 1. The LP-SeNPs have antagonistic activity against all the test pathogens. The antagonistic activity of LP-SeNPs ranged from 6.0 – 11.1 mm, 12.1 to 13.2 mm, 0.0 – 9.0 mm, 0.00 to 10.1 mm, and 0.00 to 8.1 mm against *Escherichia coli*, *Salmonella arizonae*, *Salmonella typhimurium* ATCC 14028, *Staphylococcus aureus* ATCC 25923, and *Staphylococcus aureus* 166 respectively. The highest activity was against *Salmonella arizonae* (11.3 mm). LP-culture had antagonistic activity only against *Salmonella arizonae* while the other test pathogens were resistant to the LP-culture. The broth medium and selenium broth medium did not have any antagonistic activity against all the test pathogens.

Table-1. Antibacterial activity (mm) of LP-SeNPs and LP-culture against some of the test pathogens.

Test Pathogen	Antagonistic activity (mm)				
	LP- culture	LP-SeNPs	BM	NaSeBM	Streptomycin
<i>Escherichia coli</i>	-	11.5	-	-	7
<i>Salmonella arizonae</i>	12.1	13.2	-	-	10.1
<i>Salmonella typhimurium</i> ATCC 14028	-	9	-	-	8
<i>Staphylococcus aureus</i> ATCC 25923	-	10.1	-	-	7.2
<i>Staphylococcus aureus</i> 166	-	8.1	-	-	7.2

Keys: LPBC – *Lactobacillus pentosus* ADET MW861694 culture: LP-SeNPs – *Lactobacillus pentosus* ADET MW861694 selenium nanoparticles: BM – Broth Medium: NaSeBM – Sodium selenite broth medium: Streptomycin – Streptomycin.

## 4. DISCUSSION

Deepening of the reddish color of the medium as selenite concentration increases may be attributed to higher reduction or detoxification efficiency of sodium selenite in the living cells as reported by Kieliszek, Błażej, Bzducha-Wróbel, and Kurcz (2016). An increase in selenite concentration has been reported to be proportional to an increase in elemental selenium production (Deng et al., 2015).

UV-Vis spectrum is the most basic and important technique for the observation, identification, and characterization of nanoparticles (Khurana & Vij, 2013). Colour change could be attributed to changes in the atomic size of the metal to nanosized which is seen absorbed in the visible region of the spectrum. The highest SPR peak of 300 nm observed at 72 hrs may be due to the formation of nano-selenium during the bio-reduction process of selenium ions. The absorbance peak of 200nm recorded during biosynthesis of LP-SeNPs is similar to that of Forootanfar et al. (2014) after the synthesis of nano-selenium using *Streptomyces microflavus* strain FSHJ31. The absorbance peak of 300nm is similar to that of Hariharan, Al-Harbi, Karuppiah, and Rajaram (2012) and Rajasree and Gayathri (2015) after the synthesis of nano-selenium by *Saccharomyces cerevisiae* and *Lactobacillus* spp.

respectively. The broad absorption band could be due to aggregations between selenium nanoparticles and this is similar to the report of Yang, Shen, Xie, Liang, and Zhang (2008).

The presence of functional groups is evidence of the contribution of biomolecules present in bacteria in the stabilization of selenium nanoparticles (Debieux et al., 2011). The –OH broad stretch of alcohol or phenol group corresponds to the report of Mallikarjuna et al. (2011). The presence of C-H, C=C, and C-O functional groups is similar to the report of Ananth, Keerthika, and Rajan (2019). The characteristic C-C and C-N functional group which indicates the presence of proteins correspond with the report of Jyoti, Baunthiyal, and Singh (2016) and Patel, Mighri, and Ajjji (2012).

Scanning Electron Microscopy and Transmission Electron Microscopy provides information about the morphology and size of the selenium nanoparticles. The spherical and uniformly distributed biosynthesized selenium nanoparticles revealed by the SEM micrograph are similar to the report of Eszenyi, Sztrik, Babka, and Prokisch (2011). SEM also revealed the presence of selenium nanoparticles around the cell membrane. This is in line with the report of Deng et al. (2015) on selenium nanoparticles found near the surface of the cell. TEM microscopy revealed the selenium nanoparticles dispersed in the aqueous solution to be a spherical shape which is similar to the SEM analysis and the TEM reports of selenium nanoparticle biosynthesized by Torres et al. (2012) using *Pantoea agglomerans*. However, the TEM micrograph shows the selenium nanoparticles' size was smaller than those revealed by SEM to be present in the cell membrane. This result is similar to the reports of Dhanjal and Cameotra (2010) for *Bacillus cereus* nanoparticles. The formation of larger SeNPs around the cell membrane may be due to the agglomeration of the nanoparticles after extrusion for the cell, causing them to lose their shape and increase in size (Torres et al., 2012).

EDX analysis is mostly used for qualitative (the type of elements) as well as quantitative (the percentage of the concentration of each element of the sample) analysis. The emission peak of elemental selenium at 1.50keV is similar to that observed for selenium nanoparticles biosynthesized by Fesharaki et al. (2010) using *Klebsiella pneumoniae*. The emission peak of 1.37keV, 11.22keV, and 12.49keV have been reported (Kora, 2018; Li et al., 2014). EDX spectrum revealed the presence of other elements such as C, O, Si, Ca, Fe, and Au with selenium atom accounting for about 24.80% of the total component. (Xu et al., 2018) reported the presence of other elements such as Ti and Cu in selenium nanoparticles synthesized by *L. casei*. The presence of Ca is similar to that found in selenium nanoparticles biosynthesized by *Klebsiella pneumoniae* (Fesharaki et al., 2010). Calcium acts as a reducing and stabilizing agent to prevent the clusters of selenium atoms from growing and to obtain stabilized nanoparticles in a colloidal suspension Mates et al. (2019). C and O peaks were also reported by Torres et al. (2012) for selenium nanoparticles biosynthesized by *Pantoea agglomerans*. Si element was reported to be present in selenium nanoparticles synthesized by *Alkaligenes faecalis*, and the presence of Au by *Bacillus megatarium* (Mishra et al., 2011). Generally, microbial synthesis of nano-selenium can lead to the insertion of some unknown compounds on the surface of nanoparticles; this is evident from their FTIR spectra as reported by Shakibaie et al. (2010a); Shakibaie, Khorramizadeh, Faramarzi, Sabzevari, and Shahverdi (2010b).

The difference in the particle size distribution of biosynthesized selenium nanoparticles may be due to the polydisperse (0.295) nature of the synthesized nanoparticles. Nanoparticles with a size of 98nm were the most frequently observed and an average diameter of 106.1nm was demonstrated for the biosynthesized selenium nanoparticles. Fernández-Llamosas, Castro, Blázquez, Díaz, and Carmona (2017) reported an average diameter of 136nm in *Vibrio natriegens* synthesized selenium nanoparticles. Avendano et al. (2016) also reported an average diameter of 266nm in *Pseudomonas putida* synthesized selenium nanoparticles.

Metal nanoparticles have been reported to exhibit excellent antibacterial activity against food pathogens (Stoimenov, Klinger, Marchin, & Klabunde, 2002). The zone of inhibition indicates the antibacterial efficiency of selenium nanoparticles against all the selected food pathogens. Similar results on the antibacterial activities of

selenium nanoparticles against *E. coli*, *Salmonella typhimurium*, and *Staphylococcus aureus* have been reported (Shoeibi & Mashreghi, 2017; Yang et al., 2009; Yang et al., 2018).

In conclusion, *Lactobacillus pentosus* culture was able to bio-reduced sodium selenite intracellularly for the biosynthesis of selenium nanoparticles with broad antibacterial activity against selected foodborne pathogens. There is, therefore, the need for more extensive studies on bio-fortification of food with selenium nanoparticles for nutrient improvement, bio-control spoilage, and food-borne pathogen and to improve the shelf-life of fermented food. There is a need to validation of intracellular and extracellular mechanisms of interaction between bacterial cells and metallic nanoparticles are important. This will further open up the field of food and biopharmaceutical Nanobiotechnology and pragmatic approach with potential applications in the food and pharmaceutical industries.

**Funding:** This study received no specific financial support.

**Competing Interests:** The authors declare that they have no competing interests.

**Acknowledgement:** All authors contributed equally to the conception and design of the study.

## REFERENCES

- Adebayo-Tayo, B., Salaam, A., & Ajibade, A. (2019). Green synthesis of silver nanoparticle using *Oscillatoria* sp. extract, its antibacterial, antibiofilm potential and cytotoxicity activity. *Heliyon*, 5(10), e02502. Available at: <https://doi.org/10.1016/j.heliyon.2019.e02502>.
- Alkammash, N. M. (2017). Synthesis of silver nanoparticles from *Artemisia sieberi* and *Calotropis procera* medical plant extracts and their characterization using SEM analysis. *Biosciences Biotechnology Research Asia*, 14(2), 521-526. Available at: <https://doi.org/10.13005/bbra/2474>.
- Alzate, A., Cañas, B., Pérez-Munguía, S., Hernández-Mendoza, H., Pérez-Conde, C., Gutiérrez, A. M., & Cámara, C. (2007). Evaluation of the inorganic selenium biotransformation in selenium-enriched yogurt by HPLC-ICP-MS. *Journal of Agricultural and Food Chemistry*, 55(24), 9776-9783. Available at: <https://doi.org/10.1021/jf071596d>.
- Alzate, A., Fernández-Fernández, A., Pérez-Conde, M., Gutiérrez, A., & Cámara, C. (2008). Comparison of biotransformation of inorganic selenium by *Lactobacillus* and *Saccharomyces* in lactic fermentation process of yogurt and kefir. *Journal of Agricultural and Food Chemistry*, 56(18), 8728-8736. Available at: <https://doi.org/10.1021/jf8013519>.
- Alzate, A., Pérez-Conde, M., Gutiérrez, A., & Cámara, C. (2010). Selenium-enriched fermented milk: A suitable dairy product to improve selenium intake in humans. *International Dairy Journal*, 20(11), 761-769. Available at: <https://doi.org/10.1016/j.idairyj.2010.05.007>.
- Ananth, A., Keerthika, V., & Rajan, M. R. (2019). Synthesis and characterization of nano selenium and its antibacterial response on some important human pathogens. *Current Science*, 116(2), 285-290.
- Andreoni, V., Luischi, M. M., Cavalca, L., Erba, D., & Ciappellano, S. (2000). Selenite tolerance and accumulation in the *Lactobacillus* species. *Annals of Microbiology*, 50(1), 77-88.
- Avendano, R., Chaves, N., Fuentes, P., Sanchez, E., Jiménez, J. I., & Chavarría, M. (2016). Production of selenium nanoparticles in *Pseudomonas putida* kt2440. *Science Reports*, 6, 37155. Available at: <https://doi.org/10.1038/srep37155>.
- Debieux, C. M., Dridge, E. J., Mueller, C. M., Splatt, P., Paszkiewicz, K., Knight, I., . . . Lewis, R. J. (2011). A bacterial process for selenium nanosphere assembly. *Proceedings of the National Academy of Sciences*, 108(33), 13480-13485. Available at: <https://doi.org/10.1073/pnas.1105959108>.
- Deng, Y., Man, C., Fan, Y., Wang, Z., Li, L., Ren, H., . . . Jiang, Y. (2015). Preparation of elemental selenium-enriched fermented milk by newly isolated *Lactobacillus brevis* from kefir grains. *International Dairy Journal*, 44, 31-36. Available at: <https://doi.org/10.1016/j.idairyj.2014.12.008>.
- Dhanjal, S., & Cameotra, S. S. (2010). Aerobic biogenesis of selenium nanospheres by *Bacillus cereus* isolated from coalmine soil. *Microbial Cell Factories*, 9(1), 1-11.

- Eszenyi, P., Sztrik, A., Babka, B., & Prokisch, J. (2011). Elemental, nano-sized (100-500 nm) selenium production by probiotic lactic acid bacteria. *International Journal of Bioscience, Biochemistry and Bioinformatics*, 1(2), 148-152. Available at: <https://doi.org/10.7763/ijbbb.2011.v1.27>.
- Fernández-Llamosas, H., Castro, L., Blázquez, M. L., Díaz, E., & Carmona, M. (2017). Speeding up bioproduction of selenium nanoparticles by using *Vibrio natriegens* as microbial factory. *Scientific Reports*, 7(1), 1-9. Available at: <https://doi.org/10.1038/s41598-017-16252-1>.
- Fesharaki, P. J., Nazari, P., Shakibaie, M., Rezaie, S., Banoei, M., Abdollahi, M., & Shahverdi, A. R. (2010). Biosynthesis of selenium nanoparticles using *Klebsiella pneumoniae* and their recovery by a simple sterilization process. *Brazilian Journal Microbiology*, 41(2), 461-466. Available at: 10.1590/S1517-83822010000200002.
- Forootanfar, H., Adeli-Sardou, M., Nikkhoo, M., Mehrabani, M., Amir-Heidari, B., Shahverdi, A. R., & Shakibaie, M. (2014). Antioxidant and cytotoxic effect of biologically synthesized selenium nanoparticles in comparison to selenium dioxide. *Journal of Trace Elements in Medicine and Biology*, 28(1), 75-79. Available at: <https://doi.org/10.1016/j.jtemb.2013.07.005>.
- Gericke, M., & Pinches, A. (2006). Biological synthesis of metal nanoparticles. *Hydrometallurgy*, 83(1-4), 132-140.
- Ghareib, M., Tahon, M. A., Saif, M. M., & Abdallah, W. E.-S. (2016). Rapid extracellular biosynthesis of silver nanoparticles by *Cunninghamella phaeospora* culture supernatant. *Iranian Journal of Pharmaceutical Research: IJPR*, 15(4), 915-924.
- Guo, Y., Pan, D., Li, H., Sun, Y., Zeng, X., & Yan, B. (2013). Antioxidant and immunomodulatory activity of selenium exopolysaccharide produced by *Lactococcus lactis* subsp. *lactis*. *Food Chemistry*, 138(1), 84-89. Available at: <https://doi.org/10.1016/j.foodchem.2012.10.029>.
- Hariharan, H., Al-Harbi, N., Karuppiah, P., & Rajaram, S. (2012). Microbial synthesis of selenium nanocomposite using *Saccharomyces cerevisiae* and its antimicrobial activity against pathogens causing nosocomial infection. *Chalcogenide Lett*, 9(12), 509-515.
- Institute of Medicine. (2000). *Dietary reference intakes for vitamin C, Vitamin E, Selenium, and Carotenoids*. Washington, DC: National Academies Press.
- Jyoti, K., Baunthiyal, M., & Singh, A. (2016). Characterization of silver nanoparticles synthesized using *Urtica dioica* Linn. leaves and their synergistic effects with antibiotics. *Journal of Radiation Research and Applied Sciences*, 9(3), 217-227. Available at: <https://doi.org/10.1016/j.jrras.2015.10.002>.
- Kato, H. (2011). Tracking nanoparticles inside cells. *Nature Nanotechnology*, 6(3), 139-140. Available at: <https://doi.org/10.1038/nnano.2011.25>.
- Khurana, J. M., & Vij, K. (2013). Nickel nanoparticles as semiheterogeneous catalyst for one-pot, three-component synthesis of 2-amino-4 H-pyrans and pyran annulated heterocyclic moieties. *Synthetic Communications*, 43(17), 2294-2304. Available at: <https://doi.org/10.1080/00397911.2012.700474>.
- Kieliszek, M., Błażej, S., Bzducha-Wróbel, A., & Kurcz, A. (2016). Effects of selenium on morphological changes in *Candida utilis* ATCC 9950 yeast cells. *Biological Trace Element Research*, 169(2), 387-393. Available at: <https://doi.org/10.1007/s12011-015-0415-3>.
- Kora, A. J. (2018). *Bacillus cereus*, selenite-reducing bacterium from contaminated lake of an industrial area: A renewable nanofactory for the synthesis of selenium nanoparticles. *Bioresources and Bioprocessing*, 5(1), 1-12. Available at: <https://doi.org/10.1186/s40643-018-0217-5>.
- Korbekandi, H., Irvani, S., & Abbasi, S. (2012). Optimization of biological synthesis of silver nanoparticles using *Lactobacillus casei* subsp. *casei*. *Journal of Chemical Technology & Biotechnology*, 87(7), 932-937. Available at: <https://doi.org/10.1002/jctb.3702>.
- Korbekandi, H., Ashari, Z., Irvani, S., & Abbasi, S. (2013). Optimization of biological synthesis of silver nanoparticles using *Fusarium oxysporum*. *Iranian Journal of Pharmaceutical Research*, 12(3), 289-298.

- Li, X., Yi, L., Jun, W., Huigang, L., & Songsheng, Q. (2002). Microcalorimetric study of *Staphylococcus aureus* growth affected by selenium compounds. *Thermochimica Acta*, 387(1), 57-61. Available at: [https://doi.org/10.1016/s0040-6031\(01\)00825-5](https://doi.org/10.1016/s0040-6031(01)00825-5)
- Li, D.-B., Cheng, Y.-Y., Wu, C., Li, W.-W., Li, N., Yang, Z.-C., . . . Yu, H.-Q. (2014). Selenite reduction by *Shewanella oneidensis* MR-1 is mediated by fumarate reductase in periplasm. *Scientific Reports*, 4(1), 1-7.
- Mallikarjuna, K., Narasimha, G., Dillip, G., Praveen, B., Shreedhar, B., Lakshmi, C. S., . . . Raju, B. D. P. (2011). Green synthesis of silver nanoparticles using *Ocimum* leaf extract and their characterization. *Digest Journal of Nanomaterials and Biostructures*, 6(1), 181-186.
- Mater, D. D., Bretigny, L., Firmesse, O., Flores, M.-J., Mogenet, A., Bresson, J.-L., & Corthier, G. (2005). *Streptococcus thermophilus* and *Lactobacillus delbrueckii* subsp. *bulgaricus* survive gastrointestinal transit of healthy volunteers consuming yogurt. *FEMS Microbiology Letters*, 250(2), 185-187.
- Mates, I., Antoniac, I., Laslo, V., Vicas, S., Brocks, M., Fritea, L., . . . Cavalu, S. (2019). Selenium nanoparticles: Production, characterization and possible applications in biomedicine and food science. *UPB Scientific Bulletin*, 81(1), 205-216.
- Mego, M., Májek, J., Končeková, R., Ebringer, L., Čierníková, S., Rauko, P., . . . Zajac, V. (2005). Intramucosal bacteria in colon cancer and their elimination by probiotic strain *Enterococcus faecium* M-74 with organic selenium. *Folia Microbiologica*, 50(5), 443-447. Available at: <https://doi.org/10.1007/bf02931427>.
- Mishra, R. R., Prajapati, S., Das, J., Dangar, T. K., Das, N., & Thatoi, H. (2011). Reduction of selenite to red elemental selenium by moderately halotolerant *Bacillus megaterium* strains isolated from Bhitarkanika mangrove soil and characterization of reduced product. *Chemosphere*, 84(9), 1231-1237. Available at: <https://doi.org/10.1016/j.chemosphere.2011.05.025>.
- Mokhtari, N., Daneshpajouh, S., Seyedbagheri, S., Atashdehghan, R., Abdi, K., Sarkar, S., . . . Shahverdi, A. R. (2009). Biological synthesis of very small silver nanoparticles by culture supernatant of *Klebsiella pneumoniae*: The effects of visible-light irradiation and the liquid mixing process. *Materials Research Bulletin*, 44(6), 1415-1421. Available at: <https://doi.org/10.1016/j.materresbull.2008.11.021>.
- Navarro-Alarcon, M., & López-Martínez, M. (2000). Essentiality of selenium in the human body: Relationship with different diseases. *Science of the Total Environment*, 249(1-3), 347-371.
- Palomo, M., Gutiérrez, A. M., Pérez-Conde, M. C., Cámara, C., & Madrid, Y. (2014). Se metallomics during lactic fermentation of Se-enriched yogurt. *Food Chemistry*, 164, 371-379. Available at: <https://doi.org/10.1016/j.foodchem.2014.05.007>.
- Patel, J. D., Mighri, F., & Ajji, A. (2012). Room temperature synthesis of aminocaproic acid-capped lead sulphide nanoparticles. *Materials Sciences and Applications*, 3(2), 125-130. Available at: <https://doi.org/10.4236/msa.2012.32020>.
- Pieniz, S., Andrezza, R., Pereira, J. Q., de Oliveira Camargo, F. A., & Brandelli, A. (2013). Production of selenium-enriched biomass by *Enterococcus durans*. *Biological Trace Element Research*, 155(3), 447-454. Available at: <https://doi.org/10.1007/s12011-013-9818-1>.
- Prabhu, S., Mohan, R., Sanhita, P., & Ravindran, R. (2014). Production of bacteriocin and biosynthesis of silver nanoparticles by lactic acid bacteria isolated from yoghurt and its antibacterial activity. *SIRJ-MBT*, 1(3), 7-14.
- Rajasree, R. S. R., & Gayathri, S. (2015). Extracellular biosynthesis of Selenium nanoparticles using some species of *Lactobacillus*. *Indian Journal of Geo-Marine Sciences*, 43(5), 766-775.
- Saifuddin, N., Wong, C., & Yasumira, A. (2009). Rapid biosynthesis of silver nanoparticles using culture supernatant of bacteria with microwave irradiation. *E-journal of Chemistry*, 6(1), 61-70. Available at: <https://doi.org/10.1155/2009/734264>.
- Scimeca, M., Bischetti, S., Lamsira, H. K., Bonfiglio, R., & Bonanno, E. (2018). Energy Dispersive X-ray (EDX) microanalysis: A powerful tool in biomedical research and diagnosis. *European Journal of Histochemistry*, 62, 2841. Available at: [10.4081/ejh.2018.2841](https://doi.org/10.4081/ejh.2018.2841).
- Shakibaie, M., Forootanfar, H., Mollazadeh-Moghaddam, K., Bagherzadeh, Z., Nafissi-Varcheh, N., Shahverdi, A. R., & Faramarzi, M. A. (2010a). Green synthesis of gold nanoparticles by the marine microalga *Tetraselmis suecica*. *Biotechnology and Applied Biochemistry*, 57(2), 71-75.

- Shakibaie, M., Khorramizadeh, M. R., Faramarzi, M. A., Sabzevari, O., & Shahverdi, A. R. (2010b). Biosynthesis and recovery of selenium nanoparticles and the effects on matrix metalloproteinase-2 expression. *Biotechnology and Applied Biochemistry*, 56(1), 7-15.
- Shivashankar, M., Premkumari, B., & Chandan, N. (2013). Biosynthesis, partial characterization and antimicrobial activities of silver nanoparticles from pleurotus species. *International Journal of Innovative in Science, Engineering, and Technology*, 2(2), 13-23.
- Shoeibi, S., & Mashreghi, M. (2017). Biosynthesis of selenium nanoparticles using *Enterococcus faecalis* and evaluation of their antibacterial activities. *Journal of Trace Elements in Medicine and Biology*, 39, 135-139. Available at: doi.org/10.1016/j.jtemb.2016.09.003.
- Stoimenov, P. K., Klinger, R. L., Marchin, G. L., & Klabunde, K. J. (2002). Metal oxide nanoparticles as bactericidal agents. *Langmuir*, 18(17), 6679-6686. Available at: https://doi.org/10.1021/la0202374.
- Torres, S., Campos, V., León, C., Rodríguez-Llamazares, S., Rojas, S., Gonzalez, M., . . . Mondaca, M. (2012). Biosynthesis of selenium nanoparticles by *Pantoea agglomerans* and their antioxidant activity. *Journal of Nanoparticle Research*, 14(11), 1-9. Available at: https://doi.org/10.1007/s11051-012-1236-3.
- Vigneshwaran, N., Ashtaputre, N., Varadarajan, P., Nachane, R., Paralikar, K., & Balasubramanya, R. (2007). Biological synthesis of silver nanoparticles using the fungus *Aspergillus flavus*. *Materials Letters*, 61(6), 1413-1418. Available at: https://doi.org/10.1016/j.matlet.2006.07.042.
- Xia, S. K., Chen, L., & Liang, J. Q. (2007). Enriched selenium and its effects on growth and biochemical composition in *Lactobacillus bulgaricus*. *Journal of Agricultural and Food Chemistry*, 55(6), 2413-2417. Available at: https://doi.org/10.1021/jf062946j.
- Xiao, Y., & Wiesner, M. R. (2012). Characterization of surface hydrophobicity of engineered nanoparticles. *Journal of Hazardous Materials*, 215, 146-151. Available at: https://doi.org/10.1016/j.jhazmat.2012.02.043.
- Xie, Y., He, Y., Irwin, P. L., Jin, T., & Shi, X. (2011). Antibacterial activity and mechanism of action of zinc oxide nanoparticles against *Campylobacter jejuni*. *Applied and Environmental Microbiology*, 77(7), 2325-2331. Available at: https://doi.org/10.1128/aem.02149-10.
- Xu, C., Guo, Y., Qiao, L., Ma, L., Cheng, Y., & Roman, A. (2018). Biogenic synthesis of novel functionalized selenium nanoparticles by *Lactobacillus casei* ATCC 393 and its protective effects on intestinal barrier dysfunction caused by enterotoxigenic *Escherichia coli* K88. *Frontiers in Microbiology*, 9, 1129. Available at: 10.3389/fmicb.2018.01129.
- Yang, L., Shen, Y., Xie, A., Liang, J., & Zhang, B. (2008). Synthesis of Se nanoparticles by using TSA ion and its photocatalytic application for decolorization of cango red under UV irradiation. *Materials Research Bulletin*, 43(3), 572-582.
- Yang, J., Huang, K., Qin, S., Wu, X., Zhao, Z., & Chen, F. (2009). Antibacterial action of selenium-enriched probiotics against pathogenic *Escherichia coli*. *Digestive Diseases and Sciences*, 54(2), 246-254.
- Yang, J., Wang, J., Yang, K., Liu, M., Qi, Y., Zhang, T., . . . Wei, X. (2018). Antibacterial activity of selenium-enriched lactic acid bacteria against common food-borne pathogens in vitro. *Journal of Dairy Science*, 101(3), 1930-1942.

Views and opinions expressed in this article are the views and opinions of the author(s). The International Journal of Biotechnology shall not be responsible or answerable for any loss, damage or liability etc. caused in relation to/arising out of the use of the content.